International Journal of Antimicrobial Agents 54 (2019) 601–609

Contents lists available at ScienceDirect

International Journal of Antimicrobial Agents

journal homepage: www.elsevier.com/locate/ijantimicag

Ursolic acid: A novel antiviral compound inhibiting rotavirus infection *in vitro*

M.J. Tohmé[a,c], M.C. Giménez[a,d], A. Peralta[e], M.I. Colombo[a], L.R. Delgui[a,b,*]

[a] IHEM, Universidad Nacional de Cuyo, CONICET, Facultad de Ciencias Médicas, Mendoza, Argentina
[b] Facultad de Ciencias Exactas y Naturales, Universidad Nacional de Cuyo, Mendoza, Argentina
[c] Facultad de Farmacia y Bioquímica, Universidad Juan Agustín Maza, Mendoza, Argentina
[d] Facultad de Veterinaria y Ciencias Ambientales, Universidad Juan Agustín Maza, Mendoza, Argentina
[e] Instituto de Biotecnología, Centro Nacional de Investigaciones Agropecuarias, INTA Castelar, CONICET, Buenos Aires, Argentina

ARTICLE INFO

Article history:
Received 6 December 2018
Accepted 21 July 2019

Editor: Philippe Colson

Keywords:
Rotavirus
Ursolic acid
Antiviral

ABSTRACT

Rotavirus is one of the leading causes of severe acute gastroenteritis in children under 5 years of age, mainly affecting developing countries. Once the disease is acquired, no specific treatment is available; as such, the development of new drugs for effective antirotaviral treatment is critical. Ursolic acid is a pentacyclic triterpenoid with antiviral activity, which has been studied extensively *in vitro* and *in vivo*. To study the potential antirotaviral activity of ursolic acid, its toxic potential for viral particles (virucidal effect) and cultured cells (cytotoxicity) was analysed. No effect on virion infectivity was observed with treatments of up to 40 μM ursolic acid, while incipient cytotoxicity started to be evident with 20 μM ursolic acid. The antiviral potential of ursolic acid was evaluated in *in-vitro* rotavirus infections, demonstrating that 10 μM ursolic acid inhibits rotavirus replication (observed by a decrease in viral titre and the level of the main viral proteins) and affects viral particle maturation (a process associated with the endoplasmic reticulum) 15 h post infection. Interestingly, ursolic acid was also found to hamper the early stages of the viral replication cycle, as a significant reduction in the number and size of viroplasms, consistent with a decrease in VP6 and NSP2 viral proteins, was observed 4 h post infection. As such, these observations demonstrate that ursolic acid exhibits antiviral activity, suggesting that this chemical could be used as a new treatment for rotavirus.

1. Introduction

Rotavirus (RV) remains one of the most significant pathogens associated with childhood diarrhoeal deaths in the vaccine era, and is estimated to cause approximately 129,000 diarrhoeal deaths in infants worldwide, of which >90% occur in countries in Africa and Asia [1]. Since 2006, two live oral antiRV vaccines have been prequalified by the World Health Organization (WHO) and are commercially available worldwide: Rotarix and RotaTeq. The incidence of diarrhoea does not differ substantially between regions, but case fatality and mortality rates are much higher in low-income countries compared with middle and high-income countries due to suboptimal performance of vaccination plans [2]. The presence of maternal antibodies, poor nutrition, environmental enteropathies, alterations in gut microbiota, micronutrient deficiency and exposure to other gut pathogens are some of the reasons affecting the impact of vaccines on child health. In this context, it is important to explore therapeutic alternatives that could aid infected children.

Ursolic acid (UA) (Fig. 1A) is a widespread, natural triterpene compound with many pharmaceutical properties. Triterpenes are composed of six isoprene units from mevalonic acid, most of them with 30 carbon atoms. According to their molecular classification, triterpenes can be divided into acyclic, monocyclic, bicyclic, tricyclic, tetracyclic and pentacyclic triterpenoids (including UA) and miscellaneous compounds [3]. Tetracyclic and pentacyclic triterpenoids are the most studied in the field of bioactive compounds extracted from medicinal plants and natural materials. In recent years, the medicinal values of pentacyclic triterpenoids have been studied increasingly because of their anti-inflammatory, antibacterial, antioxidant, antitumour and antiviral effects, amongst others [4]. UA is a pentacyclic triterpene carboxylic acid present as a free acid or as an aglycone part of saponins [5]. To date, the most remarkable application of UA is as an anticancer agent. UA is currently undergoing phase I trials to evaluate its safety and adverse

* Corresponding author. Address: IHEM, Universidad Nacional de Cuyo, CONICET, Facultad de Ciencias Médicas, Av, Libertador 80, Mendoza, Argentina, CP 5500.
E-mail addresses: ldelgui@fcm.uncu.edu.ar, ldelgui@mendoza-conicet.gob.ar (L.R. Delgui).

https://doi.org/10.1016/j.ijantimicag.2019.07.015
0924-8579/

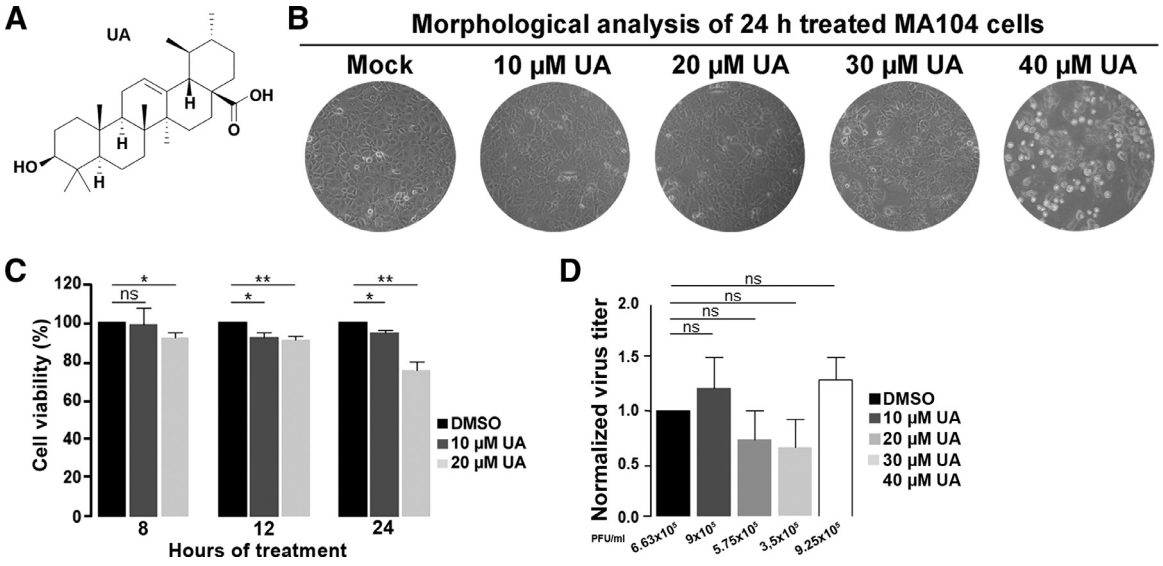

Fig. 1. Analysis of the viability of MA104 cells and virucidal effect of ursolic acid (UA). (A) UA chemical structure. (B) MA104 cells were grown in an M6 multi-well plate to 100% confluence and treated with the vehicle [dimethyl sulfoxide (DMSO)] or 10, 20, 30 or 40 µM UA in Dulbeccoś modified Eagle medium (DMEM) for 24 h. The cytotoxic effect was first evaluated *in vitro* by direct observation using an inverted light microscope. (C) MA104 cells were grown in an M96 multi-well plate to 100% confluence and treated with DMSO, 10 or 20 µM UA in DMEM in the presence of 1 µg/mL trypsin for 8, 12 and 24 h. At each time point, cellular viability was determined by Alamar blue assay as described in the text. The bar graphic represents the statistically analysed data out of three independent experiments employing Student's *t*-test: $^{*}P<0.05$, $^{**}P<0.01$ and $^{***}P<0.001$. (D) Trypsin-activated RV SA11 strain virus suspensions were incubated for 1 h at 37°C with DMSO or 10, 20, 30 or 40 µM UA and after serial dilutions, titres were determined by plaque-forming assay as described in the text. The bar graphic represents the statistically analysed data out of three independent experiments employing Student's *t*-test. PFU, plaque-forming unit.

effects in patients with solid tumours. In addition, UA exhibits antimicrobial features against numerous strains of bacteria, human immunodeficiency virus [6], hepatitis C virus [7] and plasmodium (a protozoa causing malaria). UA has been shown to have positive effects *in vitro* and *in vivo* on glucose and lipid metabolism, body weight and visceral fat usually altered in metabolic syndrome [8]. These observations, together with those demonstrating the role of lipid droplets in RV replication [9], constituted the authors' rationale to study UA as an antirotaviral compound.

UA was found to have antiviral activity at 15 h post infection (p.i.), while no virucidal effect was observed on the viral particles. The steps of the viral cycle affected were analysed, and UA was found to hamper the early stages of the replication cycle as a significant reduction in the number and size of viroplasms was observed at 4 h p.i. Taken together, these results constitute the first platform for further study of UA as an antiviral compound and its mechanism of action.

2. Materials and methods

2.1. Cell culture conditions and viruses

Epithelial monkey kidney cells (MA104 ATCC CRL-2378.1) from the Virology Institute [Instituto Nacional de Tecnología Agropecuaria (INTA), Castelar, Argentina] and NSP5-EGFP MA104 cells provided by Dr Burrone (International Centre for Genetic Engineering and Biotechnology, Rome, Italy) [10] were grown in Dulbeccoś modified Eagle medium (DMEM; Thermo Fisher Scientific. Waltham, MA, USA) containing 10% fetal bovine serum (Natocor, Argentina) at 37°C in 5% CO_2.

The SA11 RV strain (VP7 and VP4 genotype G3P5 [2]) was provided by the Biotechnology Institute (INTA). For stock production, RV viruses were activated with 20 µg/mL trypsin (Sigma-Aldrich-Merck, Argentina) at 37°C for 30 min prior to the infection of 3-day-old confluent MA104 monolayers at a multiplicity of infection (MOI) of 0.05 plaque-forming units per cell (PFU/cell). One hour after adsorption at 37°C, DMEM containing 1 µg/mL trypsin was added and left until the full cytopathic effect was observed. Viruses were purified using 10% polyethylene glycol (Sigma-Aldrich-Merck) and 2.3% ClNa as described previously [11].

2.2. Drug treatments and antibodies

UA, dimethyl sulfoxide (DMSO), methyl-ß-cyclodextrin (MßCD) and 18-ß-glycyrrhethinic acid (18ß-GRA) were purchased from Sigma-Aldrich-Merck, and Brefeldin A (BFA) was purchased from Thermo Fisher Scientific, and used in accordance with the manufacturers' instructions. For Western blot analysis, rabbit anti-SA11 specific serum was provided by the Biotechnology Institute (INTA), and rabbit anti-NSP2 serum was provided by the group of J.M. Rodriguez and D. Luque (CNM, ISCIII, Madrid, Spain). Mouse antivinculin and anti-β-actin antibodies and horseradish peroxidase (HRP)-conjugated anti-rabbit and anti-mouse secondary antibodies were purchased from Sigma-Aldrich-Merck. For viral titration by fluorescent focus assay, mouse anti-VP6 monoclonal antibody was purchased from Santa Cruz Biotechnology (Argentina), and goat anti-mouse secondary antibody conjugated with Alexa Fluor 488 and Hoechst 33342 was purchased from Molecular Probes (Thermo Fisher Scientific).

2.3. Cytotoxicity and viability assays

MA104 cells were incubated for 24 h with 10, 20, 30 and 40 µM of UA or DMSO in DMEM. After treatment, the cells were analysed by direct observation using an inverted microscope (Olympus CKX41). Alamar blue dye reagent (Thermo Fisher Scientific) was used to quantify the viability of UA-treated cells. Two concentrations of UA were tested: 10 µM and 20 µM. MA104 cells were grown in an M96 multi-well plate and treated with UA or DMSO for 8, 12 and 24 h in the presence of 1 µg/mL trypsin. Alamar blue dye reagent was added and incubated for 4 h; subsequently, the spectrophotometric signal was measured in each condition using a Multiskan FC photometer.

2.4. SDS-Page and Western blot

Mock or infected MA104 cells were mixed with Laemmliś sample buffer and heated at 95°C for 10 min prior to separation by electrophoresis, employing a 12% polyacrylamide gel, and then transferred to Hybond-ECL nitrocellulose membranes (GE Healthcare, Argentina). The membranes were blocked for 1 h with 5% non-fat milk in phosphate buffered saline (PBS) and incubated with primary antibodies [anti-SA11 (1:500), anti-VP6 (1:500), anti-NSP2 (1:500), anti-vinculin (1:1500) or anti-ß-actin (1:5000)] overnight at 4°C. After washing with PBS-Tween 0.05%, membranes were incubated for 1 h 30 min at room temperature (RT) with the corresponding HRP-conjugated secondary antibodies. Immunoreactive bands were detected using an enhanced chemiluminescence detection kit from Millipore (Argentina). Data were collected with a LAS-4000 imaging system (Fujifilm, Minato, Japan). The intensity of the bands from three independent experiments was quantified using Adobe Photoshop CS5 software.

2.5. Virus titration

2.5.1. Titration by immunofluorescence focus assay and by plaque-forming assay

MA104 cells were grown on cover slips in 24 multi-well plates up to confluence and infected with 10-fold serial dilutions of RV. After viral adsorption, viral inoculums were removed and fresh media was added for the immunofluorescence focus assay (IFA), following the protocol described in the 'Manual of rotavirus detection and characterization methods' [12]. Fluorescent foci were counted employing a Nikon TE 2000 fluorescence microscope. The viral titres were estimated as focus-forming units per mL as described previously [13]. For the plaque-forming assay (PFA), after viral adsorption, cells were overlaid with a 1:1 mixture of DMEM 2X and 1.4% low melting point agarose (Thermo Fisher Scientific), supplemented with 1 µg/mL trypsin, and maintained for 7 days at 37°C. Afterwards, cells were fixed with 10% formaldehyde (Anedra, Research S.A. Argentina) for 1 h. The semi-solid medium was removed, and the monolayers were stained with crystal violet 1% aqueous solution for 15 min. The plaques were counted to determine the viral titre in PFU/mL, as described previously [14].

2.6. Virucidal assay

For the virucidal assay, 1×10^5 PFU were trypsin activated and incubated with 10, 20, 30 or 40 µM UA or DMSO for 1 h at 37°C. Both DMSO- and UA-treated viral samples were diluted to a final volume of 200 µL in fresh DMEM, and employed for viral titration by PFA.

2.7. Total antiviral assay

Confluent MA104 cells were pre-treated with 10 µM UA or DMSO for 1 h before infection with trypsin-activated RV at a MOI of 0.1, 1 or 2 PFU/cell. After adsorption, viral inoculums were removed and cells were maintained in culture media containing 10 µM UA or DMSO, supplemented with 1 µg/mL trypsin. At 15 h p.i., the supernatants were collected to perform extracellular virus titration, and cellular pellets were harvested and disrupted by three freeze–thaw cycles, and clarified by centrifugation for intracellular virus titration by PFA. The intracellular relative amounts of VP6 and VP7 proteins were analysed by Western blot.

2.8. Early and late stages of RV replication cycle assays

2.8.1. Quantification of viral proteins and viroplasms at early stages of infection

MA104 cells were pre-treated with DMSO, 10 µM UA or 10 mM MßCD for 1 h at 37°C and infected with trypsin-activated RV at an MOI of 2 PFU/cell. The inhibitors and control vehicle were maintained during viral adsorption. The viral inoculums were removed and DMEM containing DMSO, 10 µM UA or 20 µM 18β-GRA was added. At 4 h p.i., MA104 cells were processed to Western blot. NSP5-EGFP MA104 cells were grown on cover slips, pre-treated and infected as described previously, and at 4 h p.i., the cells were fixed with 4% paraformaldehyde for 15 min at RT and mounted in Mowiol-Hoechst (1 µg/mL). Images were obtained with an Olympus FV-1000 laser scanning confocal microscope, and the number and size of viroplasms were counted in 150 cells of each condition from three independent experiments, and quantified using Image J software.

2.8.2. Quantification of viral yield at early and late stages of infection

For early stages of RV infection, confluent MA104 cells were pre-treated and infected as described. At 4 h p.i., the media was replaced by fresh DMEM without inhibitors, and the cells were incubated until 15 h p.i. For late stages of RV infection, confluent MA104 monolayers were infected with trypsin-activated RV at an MOI of 2 PFU/cell. After viral adsorption, the inoculums were removed and fresh medium was added. At 4 h p.i., the media was replaced by DMEM containing DMSO, 10 µM UA or 5 µg/mL BFA, and the infection was left to proceed up to 15 h. The supernatants were collected to perform extracellular virus titration, and cellular pellets were processed for intracellular virus titration by PFA.

2.9. Transmission electron microscopy

MA104 cells were grown in 100-mm tissue culture dishes up to confluence, pre-treated and infected as described above. At 15 h p.i., the cell monolayers were fixed for 1 h at RT with 2.5% glutaraldehyde in 0.1 M sodium cacodylate buffer at pH 7.4. Next, the samples were post-fixed in 2% osmium tetroxide in 0.1 M sodium cacodylate buffer (pH 7.4) for 1 h at RT, dehydrated with acetone, embedded in a low-viscosity Spurr resin and polymerized at 56°C for 48 h. Ultrathin sections were prepared using a Leica Ultracut R (Leica Microsystems, Wetzlar, Germany). Finally, sections of 60–100 nm were contrasted with 2% uranyl acetate/0.5% plumb citrate and viewed under a Zeiss 900 electron microscope (Oberkochen, Germany) adapted with a high-resolution CCD camera (Gatan SC1000). To quantify enveloped and non-enveloped RV viral particles, 12 images of each condition were analysed by counting the viral structures and differentiating them into enveloped and non-enveloped as described by Poruchynsky et al. [15,16]. The enveloped/non-enveloped particle ratios were determined.

2.10. Statistical analysis

Statistical analyses were performed using Student's *t*-test for unpaired data from three independent experiments. Data were expressed as mean ± standard deviation, with *P* values of $\leq$0.05, $\leq$0.01 and $\leq$0.001.

3. Results

3.1. UA is not cytotoxic for MA104 cells at 10 µM

To define the range of non-cytotoxic concentrations of UA in MA104 cells, 10, 20, 30 or 40 µM UA or DMSO were added to the culture media and the morphology of cell monolayers was

analysed using an inverted microscope at 24 h post treatment. Concentrations ≥ 20 μM UA were noted to affect the attachment of MA104 cells (Fig. 1B). Two concentrations of UA were tested and viability was measured in each condition, employing Alamar blue stain reagent to evaluate the metabolic activity of MA104 cells. So, 10 and 20 μM UA or DMSO were assayed with 1 μg/mL trypsin in each condition for 8, 12 and 24 h of treatment. While a pronounced decrease in cell viability was observed 24 h post treatment in cells treated with 20 μM UA, MA104 cells treated with 10 μM UA remained 90% viable (Fig. 1C) (DMSO: 100.0 ± 0.0004997; 10 μM UA: 94.31 ± 1.210). As such, 10 μM UA was employed in further antiviral assays.

3.2. UA does not have a virucidal effect on RV particles

Trypsin-activated RV virions were incubated with 10, 20, 30 or 40 μM UA or DMSO for 1 h at 37°C. Viral suspensions were diluted and titrated by PFA. No significant differences in RV yields were observed in RV pre-treated with UA (Fig. 1D) (DMSO: 1; 10 μM UA: 1.212 ± 0.2885; 20 μM UA: 0.7308 ± 0.2692; 30 μM UA: 0.6615 ± 0.2615; 40 μM UA: 1.288 ± 0.2115). No direct virucidal effect was observed when infective RV virions were pre-treated with UA.

3.3. UA has an antiviral effect in RV infections

Two concentrations of UA were tested to identify a dose-dependent antiviral activity. MA104 cells were pre-treated with 5 or 10 μM UA or DMSO for 1 h, and infected with trypsin-activated RV at an MOI of 0.1 PFU/cell. UA or DMSO was added to the cell culture media during the viral adsorption and post-adsorption stages. The viral progeny generated at 15 h p.i. was analysed by immunofluorescence focus assay. The results showed that the presence of 5 μM UA did not cause a significant difference in the infective progeny yield of RV, while 10 μM UA significantly decreased intra- and extracellular infective progeny (Fig. 2A) (DMSO 10 μM intracellular: 1; UA 10 μM intracellular: 0.1867 ± 0.06839; DMSO 10 μM extracellular: 1; UA 10 μM extracellular: 0.2500 ± 0.1250). Additionally, a non-significant difference in viral protein levels was observed in cells treated with 5 μM UA, while the presence of 10 μM UA caused a significant decrease in VP6 and VP7 accumulation in infected cells (Fig. 2B) (VP6 DMSO 10 μM: 1; VP6 UA 10 μM: 0.5533 ± 0.1291; VP7 UA 10 μM: 0.4900 ± 0.1290). Higher MOIs were used to test if the antiviral effect achieved by UA was also observed when higher concentrations of infective particles were used. MA104 confluent monolayers were pre-treated with 10 μM UA or DMSO and infected with RV at a MOI of 0.1, 1 or 2 PFU/cell. When 10 μM UA was present in the culture media, the cytopathic effect was markedly reduced at all MOIs tested (Fig. 2C). To define this difference quantitatively, viruses were titrated by PFA. As expected, the treatment with 10 μM UA resulted in a significant decrease in RV yield compared with the control conditions, with a more pronounced reduction in RV yield when increasing the MOI (Fig. 2D) (DMSO MOI 0.1: 1; UA MOI 0.1: 0.4100 ± 0.07234; DMSO MOI 1: 1; UA MOI 1: 0.3417 ± 0.05465; DMSO MOI 2: 1; UA MOI 2: 0.2850 ± 0.03123). Finally, the accumulation of VP6 was evaluated by Western blot analysis. Treatment with 10 μM UA was found to cause a significant reduction in intracellular VP6 levels at 15 h p.i., even when the MOI was as high as 2 PFU/cell (Fig. 2E) (DMSO MOI 0.1: 1; UA MOI 0.1: 0.6750 ± 0.0650; DMSO MOI 1: 1; UA MOI 1: 0.4050 ± 0.1750; DMSO MOI 2: 1; UA MOI 2: 0.4400 ± 0.07000) Taken together, these results reinforce the notion that 10 μM UA has an antiviral effect in RV infections, both at a low MOI (0.1) or higher MOI (2) and in a dose-dependent manner, demonstrated by a reduction in virus yield and a decrease in the intracellular level of the main RV structural proteins, VP6 and VP7.

Finally, in order to analyse the ultrastructural phenotype of viral particles produced in MA104 cells after UA treatment, the cells were pre-treated with 10 μM UA or DMSO and infected with an MOI of 0.1 PFU/mL as described above. At 15 h p.i., the infected cells were processed and analysed by transmission electron microscopy. As expected, a higher number of total viral particles was observed in the control condition compared with the UA-treated condition. It was also feasible to identify 'enveloped' immature [i.e. membrane enveloped particles (MEPs)] (intermediaries in the RV cycle) and 'non-enveloped' mature particles [i.e. triple layer particles (TLPs)] (Fig. 3). Therefore, both types of structures were determined quantitatively in UA- and DMSO-treated cells to obtain an immature/mature particle ratio for each condition. An unbalanced ratio was observed after treatment with 10 μM UA, indicating a prevalence of MEPs inside the endoplasmic reticulum (ER) compared with the control (bottom of Fig. 3). This latter observation suggested an accumulation of enveloped particles within the ER lumen in UA-treated cells, leading the authors to consider the impact of UA on virus maturation.

3.4. UA affects early stages of the RV replication cycle

The infectious cycle of RV was divided into two stages: (i) 'early stages' from attachment to viroplasm formation; and (ii) 'late stages' including progeny maturation and egress [17]. MßCD and 18ß-GRA were used as positive controls of inhibition of early stages, and BFA for late stages of the viral infectious cycle [18–20]. In order to assess the impact of UA treatment in early stages of the RV infectious cycle, viral protein accumulation and viroplasm formation was evaluated at 4 h p.i. in the presence or absence of the compounds. MA104 cells were pre-treated with DMSO, 10 μM UA or 10 mM MßCD, and infected at an MOI of 2 PFU/cell. At 1 h post adsorption, viral inoculums were removed and fresh medium was added with DMSO, 10 μM UA or 20 μM 18-βGRA. At 4 h p.i., the intracellular levels of a structural (VP6) and non-structural (NSP2) RV protein were evaluated in each condition, observing a significant decrease in VP6 and NSP2 accumulation in UA-treated cells. Treatment of the cells with the inhibitors, MβCD and 18-βGRA, caused a drastic decrease in viral protein accumulation of infected cells (Fig. 4A) (VP6 DMSO: 1; VP6 UA: 0.6578 ± 0.08257; VP6 MβCD and 18-βGRA: 0.07257 ± 0.01357; NSP2 DMSO: 1; NSP2 UA: 0.7759 ± 0.04212; NSP2 MβCD and 18-βGRA: 0.1101 ± 0.03317). NSP5-EGFP MA104 cells were used to analyse viroplasm formation in UA-treated cells. The cells were treated and infected as described, and the number and size of RV viroplasms were analysed at 4 h p.i. UA-treated and infected NSP5-EGFP MA104 cells showed a significant decrease in the number and size of viroplasms compared with control-infected cells (Fig. 4B) (size of viroplasms – DMSO: 0.9543 ± 0.02708; UA: 0.5099 ± 0.01774; MβCD and 18-βGRA: 0.09171 ± 0.01369; number of viroplasms – DMSO: 12.52 ± 0.6029; UA: 6.427 ± 0.4831; MβCD and 18-βGRA: 2.676 ± 0.2490). Finally, to evaluate if the generation of a new RV infective progeny was affected, MA104 cells were pre-treated and infected as described. At 4 h p.i., the media containing the inhibitors was removed and replaced by fresh DMEM to reach 15 h incubation. A significant decrease in viral yield in both UA- and MβCD-treated conditions was observed (Fig. 5A) (intracellular DMSO:1; UA 10 μM: 0.5167 ± 0.01667; MβCD: 0.4167 ± 0.1500; extracellular DMSO: 1; UA 10 μM: 0.2861 ± 0.06389; MβCD: 0.04064 ± 0.02970).

To evaluate the possible effect of UA in late stages of the RV infectious cycle, virus yields were determined by PFA. MA104 cells were infected as described. In contrast to the inhibitory effect observed in BFA-treated cells, UA did not cause an inhibitory effect in the late stages of the RV cycle (Fig. 5B) (intracellular DMSO: 1; UA 10 μM: 0.6018 ± 0.3968; BFA: 0.6791 ± 0.07907; extracellular

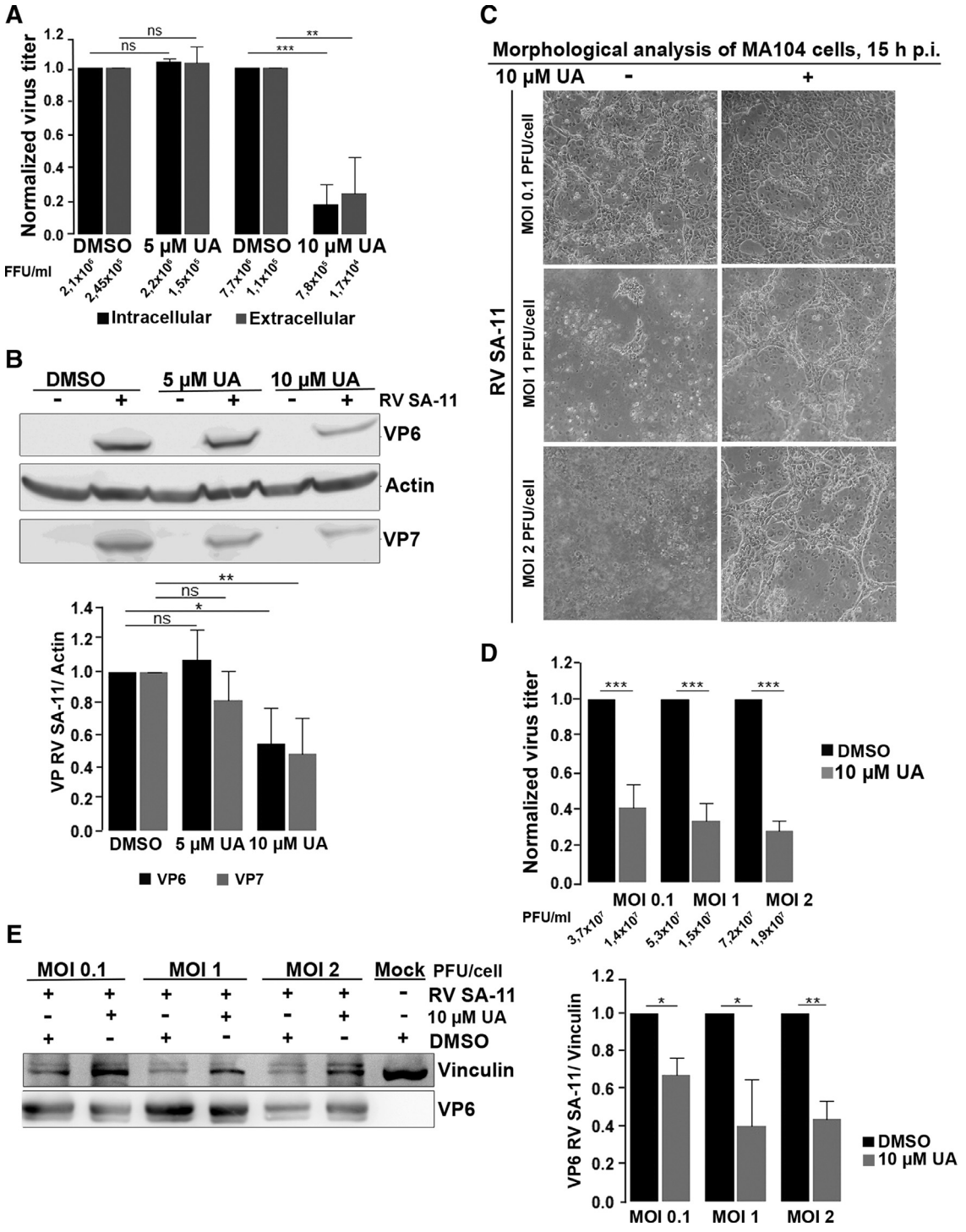

Fig. 2. Ursolic acid (UA) inhibits rotavirus (RV) replication. (A) MA104 cells were grown in an M6 multi-well plate to 100% confluence, pre-treated with dimethyl sulfoxide (DMSO), 5 or 10 µM UA for 1 h and infected with trypsin-activated RV SA11 strain at a multiplicity of infection (MOI) of 0.1 plaque-forming units (PFU)/cell in the presence of the compounds. After 1 h of viral adsorption, the viral inoculum was removed and the infection was left to proceed in the presence of UA. At 15 h post infection, the supernatants were collected for extracellular virus titration, and cellular pellets were processed for intracellular virus titration by immunofluorescence focus assay as described in the text. The bar graphic represents the statistically analysed data out of three independent experiments performed ($^{**}P<0.01$ and $^{***}P<0.001$). (B) MA104 cells were grown in an M6 multi-well plate to 100% confluence, pre-treated with DMSO, 5 or 10 µM UA for 1 h and infected with trypsin-activated RV SA11 strain at an MOI of 0.1 PFU/cell in the presence of the compounds. After 1 h of viral adsorption, the viral inoculum was removed and the infection was left to proceed in the presence of UA. At 15 h post infection, the relative amounts of intracellular VP6 and VP7 RV proteins were analysed by Western blot as described in the text. Corresponding horseradish-peroxidase-conjugated anti-mouse and anti-rabbit secondary antibodies were used to detect immunoreactive bands using a chemiluminiscence detection kit. A representative experiment from three independent experiments is shown, and quantitative data are represented in the normalized bar graphic with statistical analysis ($^{*}P<0.05$ and $^{**}P<0.01$). (C) MA104 cells were grown in an M6 multi-well plate to 100% confluence, pre-treated with DMSO or 10 µM UA for 1 h and infected with trypsin-activated RV SA11 strain at an MOI of 0.1, 1 or 2 PFU/cell, respectively. A cytopathic effect was evaluated 15 h post infection *in vitro* by direct observation using an inverted light microscope. (D) All virus produced 15 h post infection as explained in (C) was titrated by plaque-forming assay as described in the text. Data are represented normalized in a bar graphic with statistical analyses ($^{***}P<0.001$). (E) MA104 cells were infected as described in (C), and the infection was left to proceed for 15 h in the presence or absence of 10 µM UA. The relative amount of intracellular VP6 RV protein was quantified by Western blot analysis, as described in the text. A representative experiment out of three experiments is shown, and quantitative data are represented in the normalized graphic with statistical analysis ($^{*}P<0.05$ and $^{**}P<0.01$). FFU, focus-forming unit.

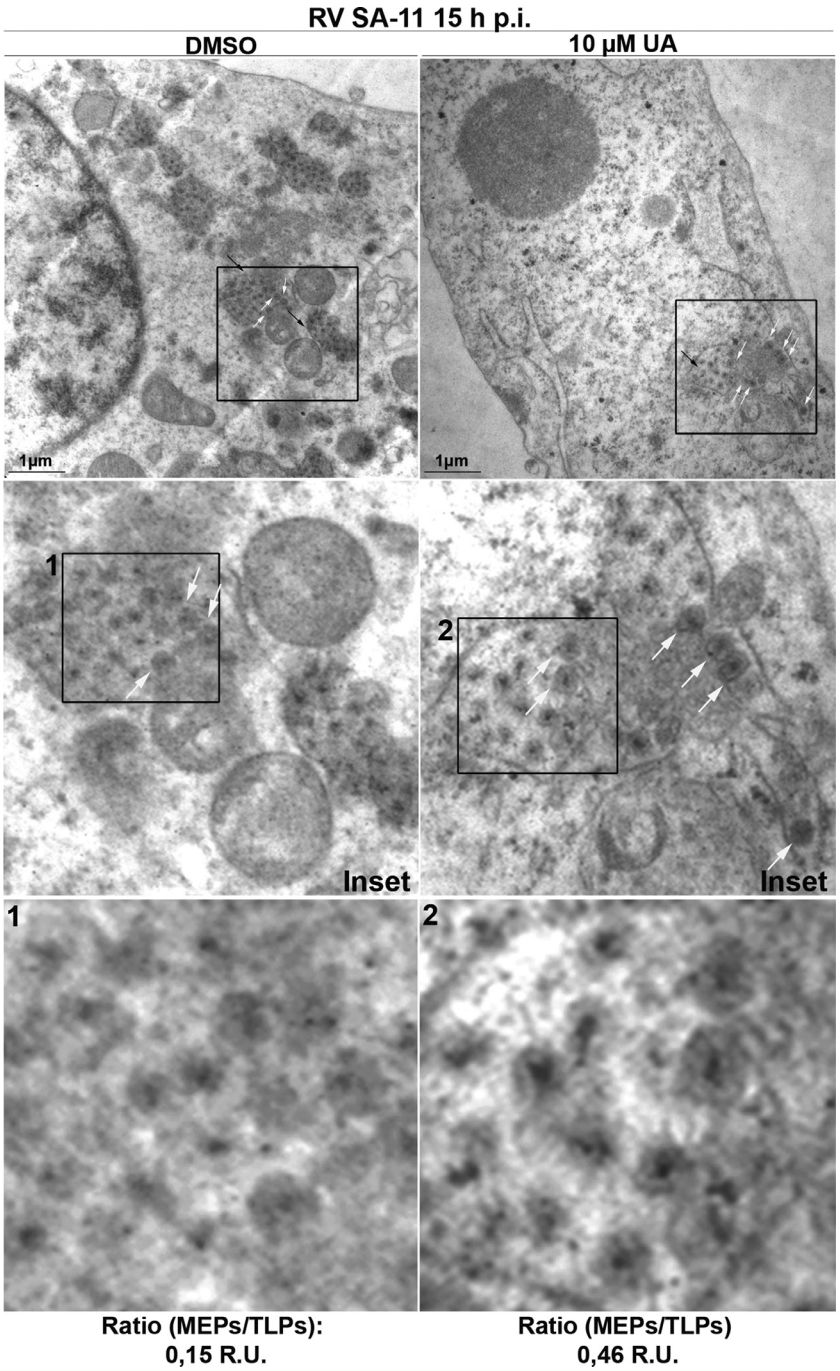

Fig. 3. Ursolic acid (UA) causes an imbalance in membrane enveloped particles (MEPs) vs non-enveloped [triple layer particles (TLPs)] rotavirus (RV) viral particles. (A) MA104 cells were grown in a 100-mm tissue culture dish to 100% confluence, pre-treated with dimethyl sulfoxide (DMSO) or 10 µM UA for 1 h and then infected with trypsin-activated RV SA11 strain at a multiplicity of infection of 0.1 plaque-forming units/cell in the presence of the compound. After 1 h of viral adsorption, the viral inoculum was removed and the infection was left to proceed in the presence of UA. At 15 h post infection (p.i.), the cells were processed for thin-section transmission electron microscopy as described in the text. Representative micrographs of cells treated with DMSO and 10 µM UA are depicted. Black arrows indicate non-enveloped viral particles and white arrows indicate enveloped particles. Scale bars represent 100 nm. Fifteen cells per condition were analysed and the ratio of MEPs to TLPs associated with the endoplasmic reticulum in DMSO- and UA-treated cells was determined as described in the text.

DMSO: 1; UA 10 µM:1.406 ± 0.4063; BFA: 0.5458 ± 0.1275). Taken together, these results indicated that UA treatment of the cells had a negative effect on viral protein accumulation and viroplasm formation in the early stages of the RV cycle.

4. Discussion

Gastroenteritis and dehydration in young children, caused by RV infections, comprise important issues in public health, particularly for low-income countries. Several compounds such as thiazolides, ML-60218, proteasome inhibitors, actin cytoskeleton inhibitors and oxysterols have been described as anti-RV, affecting different stages of the RV infectious cycle [21–24]. UA caused a significant decrease in the intracellular levels of RV viral proteins and in the production of new RV progeny when added before and during the infectious cycle, an observation that became clear with simple analysis of the cytopathic effect of UA-treated cells vs control cells. To further understand the UA-mediated anti-RV

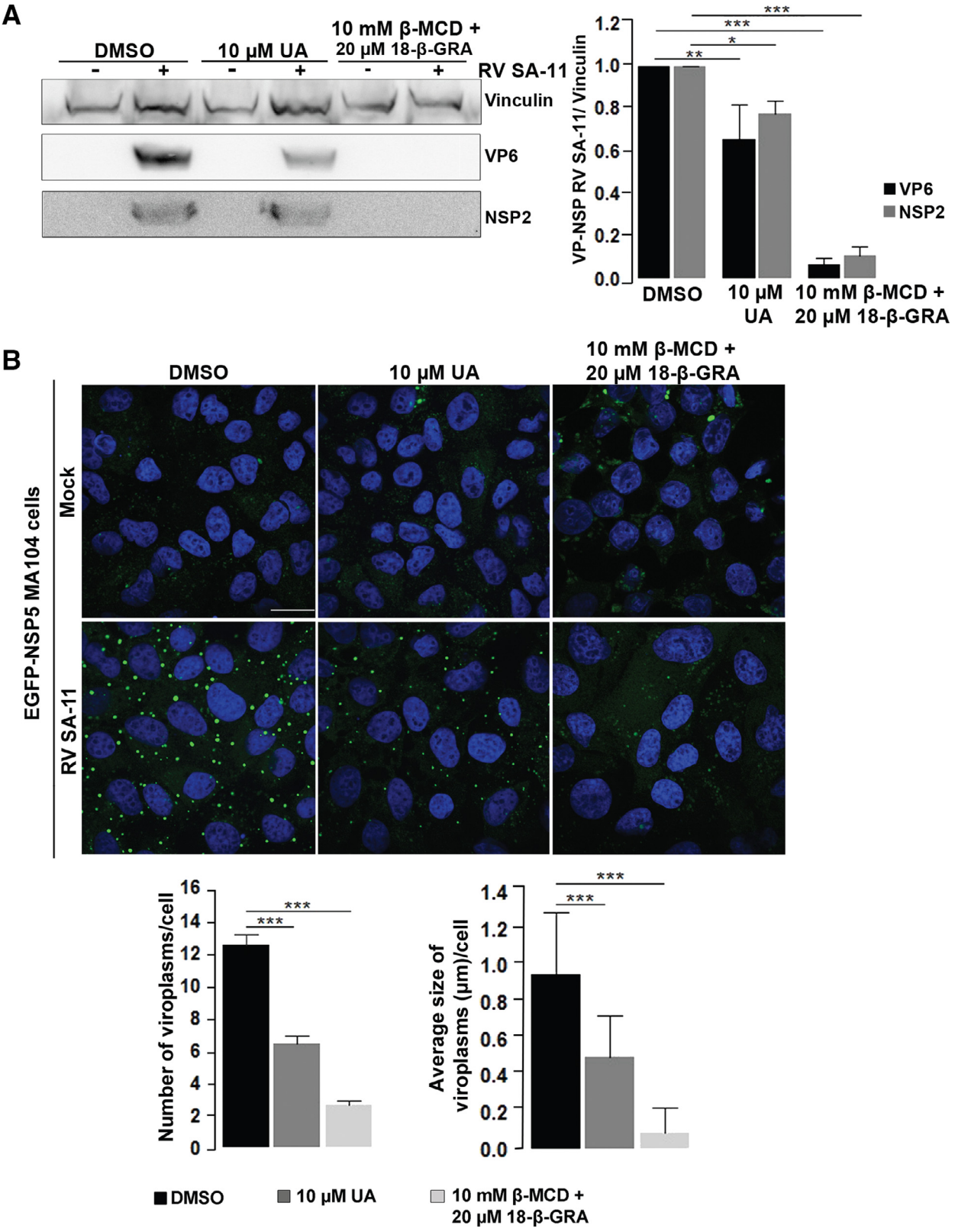

Fig. 4. Ursolic acid (UA) affects both viroplasm formation/maturation and viral protein synthesis. (A) MA104 cells were grown in an M6 multi-well plate to 100% confluence, pre-treated with dimethyl sulfoxide (DMSO), 10 μM UA or 10 mM methyl-ß-ciclodextrin (MßCD) for 1 h and infected with trypsin-activated RV SA11 strain at a multiplicity of infection of 2 plaque-forming units/cell for 1 h in presence of the drugs. The medium was removed and replaced by fresh Dulbeccoś modified Eagle medium with DMSO, 10 μM UA or 20 μM 18-β-glycyrrhetinicacid (18-β-GRA), respectively. At 4 h post infection, the relative amounts of VP6 and NSP2 were quantified by Western blot analysis as described in the text. A representative experiment out of three is shown and quantitative data are represented in the normalized graphic with statistical analysis ($^{*}P<0.05$, $^{**}P<0.01$ and $^{***}P<0.001$). (B) NSP5-EGFP MA104 cells were grown on cover slips in an M24 multi-well plate to 100% confluence, pre-treated and infected as described in (A). At 4 h post infection, the cells were fixed and observed by fluorescence confocal microscopy. The number and average size of viroplasms were quantified using MacBiophotonics ImageJ. In total, 150 cells for each condition were counted from three independent experiments, and the quantitative data are represented in the graphics with statistical analysis ($^{***}P<0.001$). All images were obtained with the same magnification and the scale bar represents 20 μm.

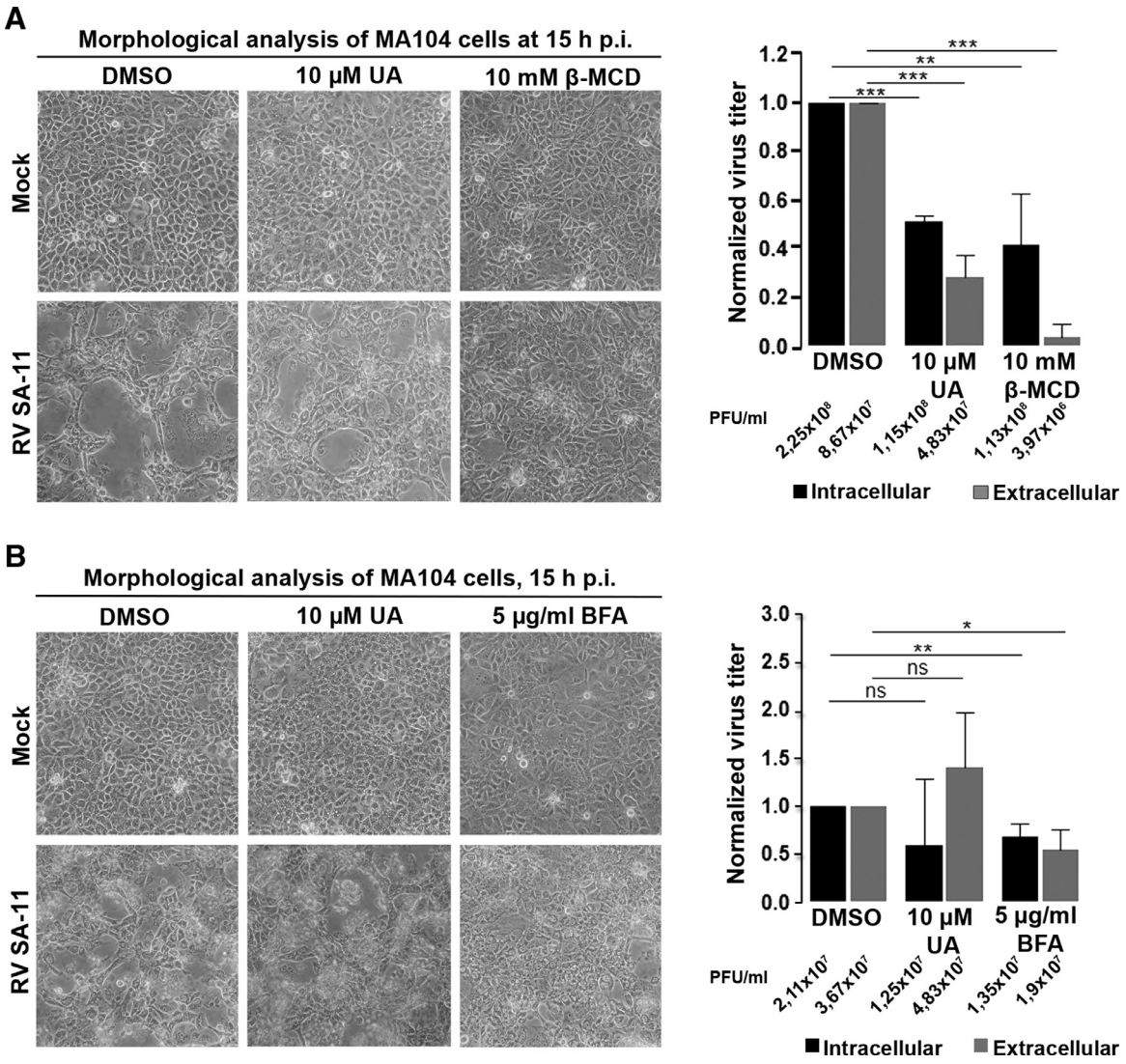

Fig. 5. Ursolic acid (UA) affects the early stages of the rotavirus (RV) replication cycle. (A) MA104 cells were grown in an M6 multi-well plate to 100% confluence, pre-treated with dimethyl sulfoxide (DMSO), 10 μM UA or 10 mM methyl-ß-ciclodextrin (MβCD) for 1 h and infected with trypsin-activated RV SA11 strain at a multiplicity of infection (MOI) of 2 plaque-forming units (PFU)/mL for 1h in the presence of the drugs. After adsorption, the viral inoculum was removed and fresh Dulbeccoś modified Eagle medium (DMEM) containing the respective drugs was added for 4 h. At 4 h post infection (p.i.), the media was replaced and the infection was left to proceed for 15 h. Cytopathic effect was evaluated *in vitro* by direct observation using an inverted light microscope. Supernatants were collected for extracellular virus titration and cellular pellets were processed for intracellular virus titration by plaque-forming assay, as described in the text. The right panel shows normalized quantitative data in a bar graphic with statistical analysis ($^{*}P<0.05$ and $^{***}P<0.001$). (B) MA104 cells were grown in an M6 multi-well plate to 100% confluence and infected with trypsin-activated RV SA11 strain at an MOI of 2 plaque-forming units/cell. After adsorption, media containing virus was removed and replaced by fresh DMEM, and 10 μM UA or 5 μg/mL Brefeldin A (BFA) was added at 4 h p.i. At 5 h p.i., the supernatants and pellets were processed as in (A). The right panel shows the normalized quantitative data in a bar graphic with statistical analysis ($^{*}P<0.05$ and $^{**}P<0.01$).

activity, the effect of UA when added for the initial 4 h of infection (early stages of infection) or at 4 h p.i. (late stages of infection) was analysed. A significant effect on viroplasm formation, decreased accumulation of structural and non-structural proteins, and inhibition of RV intra- and extracellular infective progeny were observed for UA during the initial 4 h of infection. In contrast, no significant effect on intra- and extracellular infective progeny yield was observed in the late stages of replication.

The authors' hypothesis relies on the impact of UA on viral entry and viroplasm formation, likely due to the effect of UA on cellular lipid metabolism. Several studies have reported the effect of UA on different biologically relevant lipids [8,25–30], and solid evidence exists regarding the role of cholesterol in RV entry, as well as the role of lipid droplets in viroplasm formation [9,31]. The reduction in viral entry caused by UA could explain the observed decrease in viral protein accumulation, viroplasm formation and infective progeny. Additionally, a negative impact on the metabolism of lipid droplets, exerted by UA, could explain the observed decrease in the number and size of viroplasms and, as a consequence, the decreased infective progeny. Experiments to corroborate these hypotheses are currently underway.

Characteristically, RV morphogenesis and maturation occur within the ER, one of the main cellular calcium (Ca^{2+}) reservoirs, required for structural stability of mature TLPs [32]. Several authors have described a mechanism by which UA may cause ER stress *in vitro*, by emptying the intraluminal Ca^{2+} reservoirs [33,34], leading to activation of the unfolded protein response [35]. It has also been described that dissipation of the ER Ca^{2+} gradient during infection affects RV maturation, arresting the process at MEP stage [16,36]. In light of these observations, it is hypothesized that when UA is present at every stage of the cycle, this has a significant effect on the ER, leading to a decrease in

Ca^{2+} intraluminal levels, misfolding of VP7 protein and incomplete glycosylation of both NSP4 and VP7, generating accumulation of MEPs and an unbalanced MEP/TLP ratio. The observation of an unbalanced immature/mature RV particle ratio when UA was present during the infectious cycle is in good agreement with this hypothesis. However, no significant effect on viral titre was noted during the late stages of viral replication, when ER-associated virus maturation and release take place. A feasible explanation is that the bulk of the viral progeny had already been produced when UA was added to the infection media. Further experiments are needed to explore this hypothesis.

Declaration of Competing Interest

None declared.

Acknowledgements

The authors wish to thank S. Milone and S. Galfré from the University Juan Agustín Maza for valuable laboratory help; A. Medero, D. Pastor and Dr. R. Militello from IHEM for valuable technical assistance; and E. Bocanegra, N. Domizio and J. Ibañez from IHEM for valuable technical assistance in electron microscopy and confocal laser scanning microscopy. Finally, the authors wish to thank the group of Javier María Rodriguez and Daniel Luque Buzo (CNM, ISCIII, Madrid, Spain) for sharing the rabbit serum anti-NSP2.

Funding

This work was supported, in part, by the National University of Cuyo; the SeCTyP 2013-2015 M006 and SeCTyP 2016-2018 M029 to L.R.D.; the 'Dr Casimiro Porras' grant from the Ministry of Science and Technology from Mendoza, Argentina to L.R.D.; and a grant from University Juan Agustín Maza (Resolution 889/12, 7-11-2011) to L.R.D. and ANPCyT PICT 2016-0528 to L.R.D.

Ethical approval

Not required.

References

[1] Troeger C, Forouzanfar M, Rao PC, Khalil I, Brown A, Reiner RC, et al. Estimates of global, regional, and national morbidity, mortality, and aetiologies of diarrhoeal diseases: a systematic analysis for the Global Burden of Disease Study 2015. Lancet Infect Dis 2017;17:909–48.
[2] Tate JE, Burton AH, Boschi-Pinto C, Parashar UD. Global, regional, and national estimates of rotavirus mortality in children. Clin Infect Dis 2016;62:96–105.
[3] Connolly JD, Hill RA. Triterpenoids. Nat Prod Rep 2010;27:79–132.
[4] Wozniak L, Skapska S, Marszalek K. Ursolic acid – a pentacyclic triterpenoid with a wide spectrum of pharmacological activities. Molecules 2015;20:20614–41.
[5] Liu J. Pharmacology of oleanolic acid and ursolic acid. J Ethnopharmacol 1995;49:57–68.
[6] Quéré L, Wenger T, Schramm HJ. Triterpenes as potential dimerization inhibitors of HIV-1 protease. Biochem Biophys Res Commun 1996;227:484–8.
[7] Kong L, Li S, Liao Q, Zhang Y, Sun R, Zhu X, et al. Oleanolic acid and ursolic acid: novel hepatitis C virus antivirals that inhibit NS5B activity. Antiviral Res 2013;98:44–53.
[8] Martínez-Abundis E, Méndez-Del Villar M, Pérez-Rubio KG, Zuñiga LY, Cortez–Navarrete M, Ramírez-Rodriguez A, et al. Novel nutraceutic therapies for the treatment of metabolic syndrome. World J Diabetes 2016;7:142–52.
[9] Crawford SE, Desselberger U. Lipid droplets form complexes with viroplasms and are crucial for rotavirus replication. Curr Opin Virol 2016;19:11–15.
[10] Eichwald C, Arnoldi F, Laimbacher AS, Schraner EM, Fraefel C, Wild P, et al. Rotavirus viroplasm fusion and perinuclear localization are dynamic processes requiring stabilized microtubules. PLoS One 2012;7:e47947.
[11] Queiroz Fontes LV, Campos GS, Beck PA, Lopez Brandao CF, Sardi SI. Precipitation of bovine rotavirus by polyethylen glycol (PEG) and its application to produce polyclonal and monoclonal antibodies. J Virol Methods 2005;123:147–53.
[12] World Health Organization Manual of rotavirus detection and characterization methods. Immunization. Vaccines Biol 2009;08:17.
[13] Payne AF, Binduga-Gajewska I, Kauffman EB, Kramer LD. Quantitation of flaviviruses by fluorescent focus assay. J Virol Methods 2006;134:183–9.
[14] Gray J., Desselberger U. Rotaviruses: methods and protocols. Methods Mol Med n.d.;34.
[15] Poruchynsky MS, Tyndall C, Both GW, Sato F, Richard Bellamy A, Atkinson PH. Deletions into an NH2-terminal hydrophobic domain result in secretion of rotavirus VP7, a resident endoplasmic reticulum membrane glycoprotein. J Cell Biol 1985;101:2199–209.
[16] Poruchynsky MS, Maass DR, Atkinson PH. Calcium depletion blocks the maturation of rotavirus by altering the oligomerization of virus-encoded proteins in the ER. J Cell Biol 1991;114:651–61.
[17] Desselberger U. Rotaviruses. Virus Res 2014;190:75–96.
[18] Guerrero CA, Zarate S, Corkidi G, Lopez S, Arias CF. Biochemical characterization of rotavirus receptors in MA104 cells. J Virol 2000;74:9362–71.
[19] Hardy ME, Hendricks JM, Paulson JM, Faunce NR. 18B-glycyrrhetinic acid inhibits rotavirus replication in culture. Virol J 2012;9:96.
[20] Mirazimi A, Von Bonsdorff C, Svensson L. Effect of brefeldin A on rotavirus assembly and oligosaccharide processing. Virology 1996;217:554–63.
[21] Eichwald C, De Lorenzo G, Schraner EM, Papa G, Bollati M, Swuec P, et al. Identification of a small molecule that compromises the structural integrity of viroplasms and rotavirus double-layered particles. J Virol 2018;92:1–16.
[22] Frazia SLa, Ciucci A, Arnorldi F, Coira M, Gianferretti P, Angelini M, et al. Thiazolides, a new class of antiviral agents effective against rotavirus infection, target viral morphogenesis, inhibiting viroplasm formation. J Virol 2013;87:11096–106.
[23] Civra A, Francese R, Gamba P, Testa G, Cagno V, Poli G, et al. 25-Hydroxycholesterol and 27-hydroxycholesterol inhibit human rotavirus infection by sequestering viral particles into late endosomes. Redox Biol 2018;19:318–30.
[24] Contin R, Arnoldi F, Mano M, Burrone OR. Rotavirus replication requires a functional proteasome for effective assembly of viroplasms. J Virol 2011;85:2781–92.
[25] Yarla NS, Bishayee A, Sethi G, Reddanna P, Kalle AM, Dhananjaya BL, et al. Targeting arachidonic acid pathway by natural products for cancer prevention and therapy. Semin Cancer Biol 2016;40–41:48–81.
[26] Zhang W, Zhu L, Jiang J. Active ingredients from natural botanicals in the treatment of obesity. Obes Rev 2014;15:957–67.
[27] Banihani S, Swedan S, Alguraan Z. Pomegranate and type 2 diabetes. Nutr Res 2013;33:341–8.
[28] Katashima CK, Silva VR, Gomes TL, Pichard C, Pimentel GD. Ursolic acid and mechanisms of actions on adipose and muscle tissue: a systematic review. Obes Rev 2017;18:700–11.
[29] Ngo SN, Williams DB, Head RJ. Rosemary and cancer prevention: preclinical perspectives. Crit Rev Food Sci Nutr 2011;51:946–54.
[30] Gautam R, Jachak SM. Recent developments in anti-inflammatory natural products. Med Res Rev 2009;29:767–820.
[31] Baker M, Prasad BVV. Rotavirus cell entry. Curr Top Microbiol Immunol 2010;343:121–48.
[32] Ruiz MC, Aristimuño OC, Díaz Y, Peña F, Chemello ME, Rojas H, et al. Intracellular disassembly of infectious rotavirus particles by depletion of Ca2+ sequestered in the endoplasmic reticulum at the end of virus cycle. Virus Res 2007;130:140–50.
[33] Shen S, Zhang Y, Zhang R, Tu X, Gong X. Ursolic acid induces autophagy in U87MG cells via ROS-dependent endoplasmic reticulum stress. Chem Biol Interact 2014;218:28–41.
[34] Zheng Q, Li P, Jin F, Yao C, Zhang G, Zang T, et al. Ursolic acid induces ER stress response to activate ASK1 – JNK signaling and induce apoptosis in human bladder cancer T24 cells. Cell Signal 2013;25:206–13.
[35] Brostrom M, Brostrom CO. Calcium dynamics and endoplasmic reticular function in the regulation of protein synthesis: implications for cell growth and adaptability. Cell Calcium 2003;34:345–63.
[36] Michelangeli F, Liprandi F, Chemello ME, Ciarlet M, Ruiz MC. Selective depletion of stored calcium by thapsigargin blocks rotavirus maturation but not the cytopathic effect. J Virol 1995;69:3838–47.